How the cell got its shape : A visco-elasto-active model of the cytoskeleton

Jocelyn ÉTIENNE[a] Atef ASNACIOS[b] Démosthène MITROSSILIS[b]
Valentina PESCHETOLA[a] Claude VERDIER[a]

a. *CNRS – Université J. Fourier Grenoble I, UMR 5588, Laboratoire Interdisciplinaire de Physique, F38402, Grenoble*
b. *CNRS – Université Diderot Paris 7, UMR 7057, Matière et Systèmes Complexes, F75205, Paris*

Résumé

Le cytosquelette des cellules vivantes est composé de polymères en constant réarrangement, par polymérisation et dépolymérisation, réticulés de façon transitoire (environ 1 seconde). Avec une structure aussi dynamique, on peut s'étonner de la capacité des cellules à conserver une forme stable sur des durées conséquentes. Nous proposons un modèle rhéologique qui prend en compte cette dynamique du cytosquelette et les moteurs moléculaires ; et apporte des réponses à ces questions.

Abstract

Living cells cytoskeleton is made of polymers which are constantly being re-modelled by polymerisation and depolymerisation, and which are bound to one another (crosslinked) through even more unstable molecules, lasting for about one second. With such a dynamic structure, one may wonder how cells can maintain a given shape over time ranges several orders of magnitude larger than the turn-over time of their constituents. We propose a rheological model which features crosslink turn-over, polymerisation and molecular motor-generated contractile forces, and provides answers to these questions.

1 Introduction

Cells are known to be able to maintain their shape and exert stress on their environment over a time scale of hours, a duration which seems to be limited only by their division cycle or their urge for finding other conditions by migration. However, it is also known that the internal structure which allows them to resist and exert stress are highly dynamic and non-permanent [1]: the lifetime of these elements, from cross-linkers to actin filaments and microtubules, ranges from a fraction of a second up to a maximum of a dozen minutes.

This elicits a very natural question: how can possibly such a changeable material maintain a constant shape and stress? If one was to unbolt and re-bolt a significant fraction of the Eiffel Tower's girders at such a rate, chances are that some of them would be disconnected altogether and fall down at some point. Even if they are stopped in their fall by the framework entanglement, and get re-bolted with adjacent girders, one imagines that the Tower will eventually collapse. So what does the cell do that prevents this collapse? Quite evidently, the cell is assisted with a crowd of workers which re-tense its structure, namely molecular motors.

Let us imagine an experiment that will hurt (somewhat) less of physiology. Consider a sample of the acto-myosin cortex of a cell, that would be fixed between two plates submitting it to an extensional constraint (figure 1). For simplicity, let us consider that this sample is sufficiently large so that no single filament spans the distance between the plates. This is actually the case in a whole cell sitting on a substrate, as no single filament spans the distance accross the cell. Thus at least part of the crosslinkers bear some of the tension in the sample. Every time one of these cross-linkers is disconnected, the actin meshwork will thus relax and extend somewhat. If there are no molecular motors present, the actin meshwork will thus yield to the extensional force at a rate which, in the first approximation, depends only on the crosslinker unbinding rate and on the force, and not on parameters such as the current distance between the plates. An observer will thus deem that the sample is a fluid, albeit a very viscous one.

Now if there are motors present, we know that they can exert a contractile stress. Thus one can imagine that, as crosslinkers unbind, the resulting local deformation will depend on the difference between the global extension and

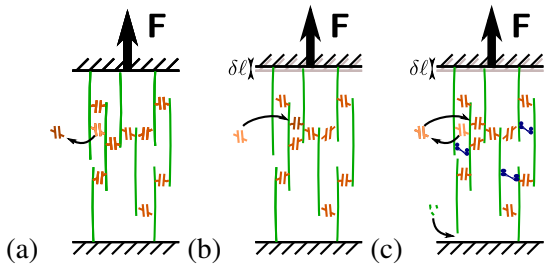

Figure 1: Modelling view of acto-myosin gel. (a) Crosslinked actin gel under extensional stress. As a crosslinker detaches, the network relaxes to situation (b). The crosslinker then rebinds, but in a relaxed state, which does not change the new equilibrium length. (c) Myosin and actin polymerisation at boundaries also affect the stress.

local motor-driven contraction this crosslinker used to resist. Thus, the acto-myosin cortex is expected to be able to sustain some level of tension equal to the total stress generated by its molecular motors.

In this paper, we develop a rheological model based on these observations. This continuous model[1] is in the line of ideas developped by Dembo [3] and Kruse [4] but in a simplified framework and with a reduced number of parameters. We test its predictions in several situations where we have performed rheometrical experiments on live cells. It is found that our simple model captures faithfully the force–deformation relations observed in experiments.

2 A visco-elasto-active model of the cell cytoskeleton

2.1 Constitutive equations

Let us consider the thought experiment above. A cross-linked network is maintained under extensional stress, as in figure 1. Cross-linkers unbind with a characteristic time τ_α, which causes the network to yield locally to the stress. These unbound cross-linkers then re-bind elsewhere in the new configuration of the network, so that the elastic modulus of the network is unchanged after this unbinding–re-binding sequence, but its configuration has changed.

We suppose that the network is very large in terms of number of crosslinks. The displacement $\delta\ell$ which results from the unbinding of one tensed crosslink is of the order σ/E, where σ is the stress and E the Young's modulus characterizing the network. Such an event occurs at a rate $1/\tau_\alpha$, where τ_α is the average lifetime of a crosslink. The strain is thus composed of a plastic component ε_p such that $\dot\varepsilon_\mathrm{p} = \sigma/(\tau_\alpha E)$ in addition to the elastic strain $\varepsilon_\mathrm{e} = \sigma/E$. The Young's modulus of the network does not change in time in this process, because unbound crosslinkers are hypothesised to rebind somewhere else (in relaxed state), so that the structure of the network, which determines its elasticity, is unchanged[2]. Thus, some simple algebra yields what turns out to be Maxwell constitutive equation:

$$\tau_\alpha\dot\sigma + \sigma = \tau_\alpha E\,\dot\varepsilon$$

If myosin is present, it will contribute to the strain rate with $\dot\varepsilon_\mathrm{my} = -c_\mathrm{my}\ell_\mathrm{my}/\tau_\mathrm{my}$ in proportion of its concentration c_my and step length ℓ_my, at its rate of binding $1/\tau_\mathrm{my}$. This generates an additional stress, and the constitutive equation becomes :

$$\tau_\alpha\dot\sigma + \sigma = \Sigma + \tau_\alpha E\,\dot\varepsilon \tag{1}$$

with $\Sigma = \frac{\tau_\alpha}{\tau_\mathrm{myo}} c_\mathrm{myo}\ell_\mathrm{myo}E$. In the absence of crosslinkers and of any external force balancing the stress of the acto-myosin network (thus $\tau_\alpha = 0$ and $\sigma = 0$), we find that the acto-myosin network will contract indefinitely with a characteristic contraction time $\tau_\mathrm{c} = \tau_\alpha E/\Sigma$. This is what is observed experimentally in non-crosslinked purified gels and is called superprecipitation [5, 6].

One may consider that there is more than one relaxation time in the actin plus crosslinkers network, possibly due to different unbinding times and complex relaxation modes [e.g. 7], yielding a set of constitutive relations for each of them.

Similarly to the tensorial extension of the Maxwell constitutive relations, the tensorial version of the visco-elasto-active constitutive relation requires the use of an objective derivative to guarantee that the relation is frame-invariant. Using the upper-convected derivative $\overset{\triangledown}{\boldsymbol{\sigma}} = \frac{\partial}{\partial t}\boldsymbol{\sigma} + \boldsymbol{u}\cdot\nabla\boldsymbol{\sigma} - (\nabla\boldsymbol{u})^T\boldsymbol{\sigma} - \boldsymbol{\sigma}(\nabla\boldsymbol{u})$, we obtain :

$$\tau_\alpha\overset{\triangledown}{\boldsymbol{\sigma}} + \boldsymbol{\sigma} = \boldsymbol{\Sigma} + \tau_\mathrm{c}\Sigma\mathbf{D}(\boldsymbol{u})$$

where $\boldsymbol{u}$ is the velocity of the actin network, and $\mathbf{D}(\boldsymbol{u}) = \frac{1}{2}(\boldsymbol{\nabla u} + \boldsymbol{\nabla u}^\mathrm{T})$ the rate of strain tensor. $\boldsymbol{\Sigma} = \Sigma\boldsymbol{I}$ if we assume an isotropic force generation.

[1] See [2] for a review of modelling approaches for living cells

[2] The same argument holds for actin treadmilling provided that the average filament length is a constant in time

2.2 Governing equations for an acto-myosin network

We consider that, in most conditions, the leading order force balance within the actomyosin cortex is between the forces it actively generates and the boundary conditions. Thus there is no bulk force to balance the stress $\boldsymbol{\sigma}$:

$$\begin{cases} \tau_\alpha \overset{\triangledown}{\boldsymbol{\sigma}} + \boldsymbol{\sigma} = \boldsymbol{\Sigma} + \tau_\mathrm{c} \Sigma \mathbf{D}(\boldsymbol{u}) & \text{(2a)} \\ \mathrm{div}\, \boldsymbol{\sigma} = \mathbf{0} & \text{(2b)} \end{cases}$$

What we obtain is a visco-elastic Maxwell-type constitutive equation (2a) with a term Σ that represents motor-generated stress in the right-hand-side, and an equilibrium equation (2b) in which there is no bulk force to balance the visco-elastic stress: thus it must be balanced by boundary conditions in our case. This model can be shown to be a particular case of the models by Dembo [3] and Kruse [4]. Of course, in some cases this model must be complemented by extra terms that we have neglected here. For instance, the round shape of cells in suspension can be recovered by considering that the cytoplasm inside the cell is under pressure. Within the acto-myosin cortex, the gradient of this pressure will balance the motor-generated stress $\boldsymbol{\sigma} = \Sigma$ in the static solution, and yield Laplace law. It is known that myosin motor-generated strain stalls at a given value of stress, however this does not have to be imposed here in the modelling: this stalling arises naturally from the constitutive equation we obtain. Indeed, if one considers e.g. a characteristic time much shorter than τ_α, Eq. 1 can be integrated in time and yields $2E(-\epsilon) = \Sigma - \sigma$, which states that the contraction $-\epsilon$ (the opposite of the extension) decreases as the stress developped $\boldsymbol{\sigma}$ increases up to a fixed stall value Σ.

2.3 Actin polymerisation

One can easily see from the sketch in figure 1 that actin treadmilling only matters at boundaries, provided that there is no net extension of the filaments and thus that the Young's modulus of the network will remain the same in time. Actin polymerisation is thus incorporated in the model simply by postulating that it creates a velocity difference at the boundary, between the velocity of the boundary itself and the velocity of the actomyosin network. This velocity difference is equal to the speed of actin polymerisation v_p.

2.4 Adhesion

Cells encountering a two-dimensional flat substrate generally adhere and spread on it. This spreading can be enhanced by an adequate functionalisation of the substrate. A simple modeling approach consist of considering that, in the plane tangential to the flat substrate, adhesion has the same properties as wall-friction in a Hele Shaw cell, therefore the model writes:

$$\begin{cases} \lambda \overset{\triangledown}{\boldsymbol{\sigma}} + \boldsymbol{\sigma} = \boldsymbol{\Sigma} + \mathbf{D}(\boldsymbol{u}) & \text{in } \Omega(t) & \text{(3a)} \\ -c_\mathrm{f} \boldsymbol{u} + \mathrm{div}\, \boldsymbol{\sigma} = 0 & \text{in } \Omega(t) & \text{(3b)} \\ \dfrac{\partial \boldsymbol{\gamma}}{\partial t} = \boldsymbol{u}(\boldsymbol{\gamma}) + u_\mathrm{p} \boldsymbol{n} & \text{for } s \in [0, |\Gamma(t)|] & \text{(3c)} \\ \boldsymbol{\sigma} \boldsymbol{n} = \boldsymbol{F} & \text{on } \Gamma(t) = \{\boldsymbol{\gamma}(t,\, s),\, s \in [0, |\Gamma(t)|]\} & \text{(3d)} \end{cases}$$

with $\lambda = \frac{\tau_\alpha}{\tau_\mathrm{c}}$, and $u_\mathrm{p} = \frac{v_p \tau_\mathrm{c}}{L_0}$. c_f is a friction coefficient nondimensionalised by $\tau_\mathrm{c}\Sigma/L_0^2$. γ tracks the position of the contour of the domain $\Omega(t)$.

3 Numerical technique

For addressing more complex geometries and non-stationary behaviours of this active material, it is necessary to resort to numerical simulations. Here we describe an original mixed formulation to solve this Maxwell-type problem.

Using the characteristics method for the objective derivative [8] with the same approach as [9], we discretise problem (3) in time and take its variational formulation. We now want to find $(\boldsymbol{\sigma}^n, \boldsymbol{u}^n)$ in $S^n \times V^n$ and $\boldsymbol{\gamma}^n$ such that:

$$\begin{cases} \left(\dfrac{\mathrm{De}}{\Delta t}+1\right)\displaystyle\int_\Omega \boldsymbol{\sigma}^n : \boldsymbol{\tau}\,\mathrm{d}x - \int_\Omega \mathbf{D}(\boldsymbol{u}^n) : \boldsymbol{\tau}\,\mathrm{d}x \\ \qquad\qquad = \displaystyle\int_\Omega \left(\boldsymbol{\Sigma} + \frac{\mathrm{De}}{\Delta t}\boldsymbol{R}\boldsymbol{\sigma}^{\boldsymbol{n-1}}\boldsymbol{R}^{\mathrm{T}}\right) : \boldsymbol{\tau}\,\mathrm{d}x \qquad \forall \boldsymbol{\tau} \in S^n & \text{(4a)} \\ -\displaystyle\int_\Omega \boldsymbol{u}^n \cdot \boldsymbol{v}\, c_{\mathrm{f}}\,\mathrm{d}x - \int_\Omega \boldsymbol{\sigma}^n : \mathbf{D}(\boldsymbol{v})\,\mathrm{d}x = -\int_\Gamma \boldsymbol{F}\cdot\boldsymbol{v}\,\mathrm{d}s \qquad \forall \boldsymbol{v} \in V^n & \text{(4b)} \\ \boldsymbol{\gamma}^n = \boldsymbol{\gamma}^{n-1} + \Delta t\left(\boldsymbol{u}^{n-1}(\boldsymbol{\gamma}^{n-1}) + u_{\mathrm{p}}\boldsymbol{n}\right) \qquad \text{for } s \in [0, |\Gamma^n|] & \text{(4c)} \end{cases}$$

where $\Gamma^n = \{\boldsymbol{\gamma}^n(s), s \in [0, s_{\max}]\}$, and Ω^n such that $\partial\Omega^n = \Gamma^n$, $S^n = \left\{\boldsymbol{\tau} \in L^2(\Omega^n)^{d(d+1)/2}\right\}$ and $V^n = \left\{\boldsymbol{v} \in H^1(\Omega^n)^d\right\}$. Let us introduce the following bilinear forms:

$$m_t(\boldsymbol{\sigma},\boldsymbol{\tau}) = \int_\Omega \boldsymbol{\sigma}:\boldsymbol{\tau}\,\mathrm{d}x,\ \forall(\boldsymbol{\sigma},\boldsymbol{\tau}) \in (S^n)^2 \qquad b(\boldsymbol{\tau},\boldsymbol{v}) = -\int_\Omega \boldsymbol{\tau}:\mathbf{D}(\boldsymbol{v})\,\mathrm{d}x,\ \forall(\boldsymbol{\tau},\boldsymbol{v}) \in S^n\times V^n$$
$$m_f(\boldsymbol{u},\boldsymbol{v}) = \int_\Omega c_{\mathrm{f}}\boldsymbol{u}\cdot\boldsymbol{v}\,\mathrm{d}x,\ \forall(\boldsymbol{u},\boldsymbol{v}) \in (V^n)^2 \qquad b_b(\boldsymbol{F},\boldsymbol{v}) = -\int_\Gamma \boldsymbol{F}\cdot\boldsymbol{v}\,\mathrm{d}s,\ \forall(\boldsymbol{\tau},\boldsymbol{v}) \in S^n\times V^n$$

The semi-discrete problem now writes:

$$\begin{cases} \text{Find } (\boldsymbol{\sigma}^n,\boldsymbol{u}^n) \in S^n\times V^n \text{ such that:} \\ \left(\dfrac{\mathrm{De}}{\Delta t}+1\right) m_t(\boldsymbol{\sigma}^n,\boldsymbol{\tau}) + b(\boldsymbol{\tau},\boldsymbol{u}^n) = m_t(\Sigma,\boldsymbol{\tau}) + \dfrac{\mathrm{De}}{\Delta t} m_t(\boldsymbol{R}\boldsymbol{\sigma}^{n-1}\boldsymbol{R}^{\mathrm{T}},\boldsymbol{\tau}) \qquad \forall\boldsymbol{\tau}\in S^n & \text{(5a)} \\ b(\boldsymbol{\sigma}^n,\boldsymbol{v}) - m_f(\boldsymbol{u}^n,\boldsymbol{v}) = b_b(\boldsymbol{F},\boldsymbol{v}) \qquad \forall\boldsymbol{v}\in V^n & \text{(5b)} \\ \boldsymbol{\gamma}^n = \boldsymbol{\gamma}^{n-1} + \Delta t\left(\boldsymbol{u}^{n-1}(\boldsymbol{\gamma}^{n-1}) + u_{\mathrm{p}}\boldsymbol{n}\right) \qquad \text{for } s\in[0,|\Gamma^n|] & \text{(5c)} \end{cases}$$

Now let us introduce a triangulation $\mathcal{T}_h^n$ of Ω^n, and the following finite element spaces:

$$S_h^n = S^n \cap \left\{\boldsymbol{\tau}_{|_K} \in P_1(K), \forall K \in \mathcal{T}_h^n\right\} \qquad V_h^n = V^n \cap \left\{\boldsymbol{\tau}_{|_K} \in P_2(K), \forall K \in \mathcal{T}_h^n\right\} \cap C^0(\Omega^n)$$

The following Riesz representers are defined over the discrete spaces:

$$m_t(\boldsymbol{\sigma}_h,\boldsymbol{\tau}_h) = \langle M_t\boldsymbol{\sigma}_h,\boldsymbol{\tau}_h\rangle,\ \forall(\boldsymbol{\sigma}_h,\boldsymbol{\tau}_h)\in(S_h^n)^2 \qquad b(\boldsymbol{\tau}_h,\boldsymbol{v}) = \langle B\boldsymbol{\tau}_h,\boldsymbol{v}\rangle,\ \forall(\boldsymbol{\tau}_h,\boldsymbol{v}_h)\in S_h^n\times V_h^n$$
$$m_f(\boldsymbol{u}_h,\boldsymbol{v}_h) = \langle M_f\boldsymbol{u}_h,\boldsymbol{v}_h\rangle,\ \forall(\boldsymbol{u}_h,\boldsymbol{v}_h)\in(V_h^n)^2 \qquad -\int_{\Gamma_h}\boldsymbol{F}\cdot\boldsymbol{v}\,\mathrm{d}s = \langle B_b\boldsymbol{\tau}_h,\boldsymbol{v}\rangle,\ \forall(\boldsymbol{\tau}_h,\boldsymbol{v}_h)\in S_h^n\times V_h^n$$

Note that if c_{f} vanishes on part of the domain, then M_f is singular. Because there is no continuity requirement for S_h^n, the Riesz-representer matrix M_t of m_t over $S_h^n\times S_h^n$ is block-diagonal and can be easily inverted. Thus, a direct solution algorithm can be written for problem (5):

$$\begin{cases} \text{Find } (\boldsymbol{\sigma}_h^n,\boldsymbol{u}_h^n) \in S_h^n\times V_h^n \text{ such that:} \\ \left(M_f + \left(1+\dfrac{\mathrm{De}}{\Delta t}\right)BM_t^{-1}B^{\mathrm{T}}\right)\boldsymbol{u}_h^n = B\boldsymbol{\Sigma} - B_b\boldsymbol{F}_h + \dfrac{\mathrm{De}}{\Delta t}B(\boldsymbol{R}_h\boldsymbol{\sigma}_h^{n-1}\boldsymbol{R}_h^{\mathrm{T}}) & \text{(6a)} \\ \boldsymbol{\sigma}_h^n = \boldsymbol{\Sigma} - M_t^{-1}B^{\mathrm{T}}\boldsymbol{u}_h^n & \text{(6b)} \\ \boldsymbol{\gamma}_h^n = \boldsymbol{\gamma}_h^{n-1} + \Delta t\left(\boldsymbol{u}_h^{n-1}(\boldsymbol{\gamma}_h^{n-1}) + u_{\mathrm{p}}\boldsymbol{n}_h\right) & \text{(6c)} \end{cases}$$

(a) 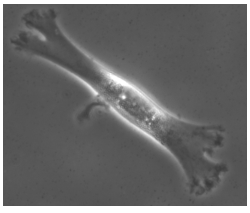 (b) 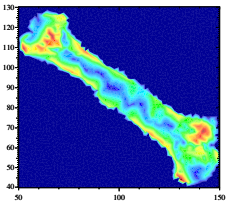 (c) 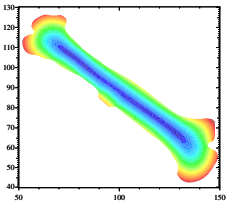

Figure 2: Force exerted by a cell on its flat substrate (seen from below). (a) Phase contrast microsopy image of the cell shape (b) Experimental results obtained by traction force microscopy [10]. (c) Numerical simulation of the present model based on the cell shape in the experiment. The distribution of force is seen to be similar in the experiment and simulation for a given shape.

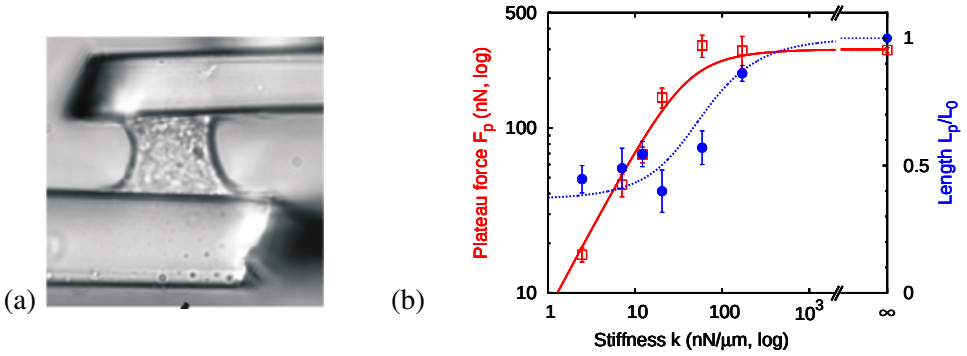

Figure 3: Comparison of model predictions for the setup in figure 1 with $F = -k(L - L_0)$ and experiments with a cell placed in a device having the same spring-like behaviour [11, 12]. (a) Experimental setup : the cell placed between the microplates deflects them, and an equilibrium length L_p is reached when the cell-generated force is balanced by the spring-like force of the device $F_p = -k(L_p - L_0)$ (b) Equilibrium length (blue) and force (red) generated experimentally by a cell (squares and circles) and in theory by the actomyosin model (curves) in a spring-like device as a function of the stiffness k of this device.

4 Predictions of the model

4.1 Cell traction force

For a given cell shape, the model predicts that the cell exerts centripetal forces of increasing magnitude as a function of the distance to the central region of the cell. The rate of increase depends on the ratio of the friction c_f and contractility Σ parameters. The predicted force field is similar to what is observed in experiments, see figure 2.

4.2 Equilibrium length in uniaxial sollicitation

We look here for solutions of the model where the unknowns are independent of time, and the shape of the cell is steady. A steady shape of the cell corresponds to the fact that the polymerisation velocity $v_p \boldsymbol{n}$ is exactly balanced by the actin velocity at the boundary $\boldsymbol{u}_{|\Gamma}$.

In the one-dimensional setting of figure 1, a unique equilibrium length is determined by the force applied at the plates. If the force is negligible, then the motor-generated contractile stress Σ in the cell can only be balanced by a dissipative stress due to a permanent contraction of the actin network, and $\sigma = 0$. An equilibrium is reached when the contraction velocity is balanced exactly by the polymerisation velocity. This happens for a length $L_e = 2\tau_\mathrm{c} v_p$. When the force increases, some internal stress σ partly balances the motor-generated stress, the actin contraction speed decreases and thus the equilibrium length increases in a hyperbolic manner, with a failure of the actomyosin network as the force approaches the motor generated stress.

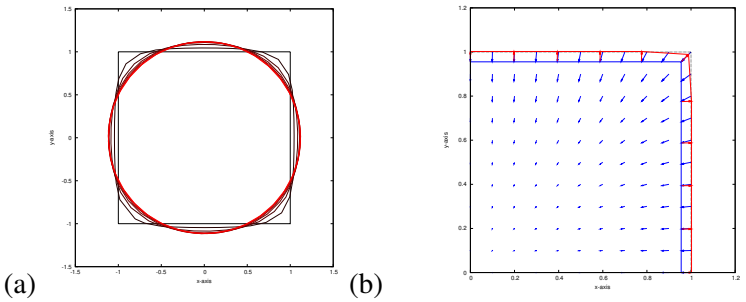

Figure 4: Equilibrium shape in 2D spreading. The initially square domain occupied by a material governed by the visco-elasto-active constitutive equation deforms until it reaches a circular shape, whose size is determined by a balance between polymerisation and adhesion-limited contraction of the material. (a) overlay of the shapes of the domain at $t = 0$, 1,... to 7, (b) velocity $\boldsymbol{u}_h$ of the material (blue arrows) and polymerisation speed (red arrows) at time $t = 0$. The shape resulting from material contraction is shown in blue (from the initial shape at $t = 0$, black dotted line) and the shape resulting from the combination contraction plus polymerisation in red. When the equilibrium shape is reached, these two phenomena still occur, and balance exactly.

If the force is length-dependent, such as the spring-like device developped in [11, 12], then there is always an equilibrium length. In figure 3 we compare experimental results of the force and length that a cell exerts in a spring-like device and theoretical predictions for the conditions shown in figure 1. Although there are essential differences in the conditions, the key fact is that both cell experiments and actomyosin model predictions exhibit a stalling stiffness above which motors tetanise, and a horizontal asymptote for a finite equilibrium length at low stiffness. Note that experimentally, the length L_0 is both the equilibrium distance between the plates of the device and the equilibrium size of the cell when in suspension.

4.3 Equilibrium shape in 2D spreading

In a polar symmetry setting, it can be shown that for some choices of the parameters, there exists an equilibrium radius R such that a circular shape of that radius is a linearly stable, steady solution of this system. A numerical example of convergence towards this solution is shown in figure 4.

This static shape is again the result of two persisting dynamic processes : although the shape $\Omega(t)$ reaches an equilibrium, the actin network undergoes perpetual centripetal flow, driven by the myosin motors. At the same time, outward-directed polymerisation at the edges exactly balances this centripetal flow. This is very reminiscent of what is observed in adhering cells, even when they are immobile, see [13].

5 Conclusions

Unlike an elastic material, the cells cytoskeleton does not have a memory of its own shape. This shape must then constantly be maintained through energy-consuming, dynamic processes that depend on external and internal conditions. The advantage of this, as we will show in a forthcoming paper, is that adaptation to a new mechanical environment begins instantaneously when external conditions are changed.

References

1. C. Verdier, J. Étienne, A. Duperray, and L. Preziosi. Review. Rheological properties of biological materials. *C. R. Physique*, 10:790–811, 2009.
2. A. Vaziri and A. Gopinath. Cell and biomolecular mechanics in silico. *Nature Materials*, 7:15–23, 2008.
3. M. Dembo and F. Harlow. Cell motion, contractile networks, and the physics of interpenetrating reactive flow. *Biophys. J.*, 50:109–121, 1986.
4. K. Kruse, J.F. Joanny, F. Jülicher, J. Prost, and K. Sekimoto. Generic theory of active polar gels: a paradigm for cytoskeletal dynamics. *Eur. Phys. J. E*, 16:5–16, 2005.
5. T. Hayashi and K. Maruyama. Myosin aggregates as a requirement for contraction and a proposal to the mechanism of contraction of actomyosin systems. *J. Biochem.*, 78:1031–1038, 1975.
6. D. Mizuno, C. Tardin, C.F. Schmidt, and F.C. MacKintosh. Nonequilibrium mechanics of active cytoskeletal networks. *Science*, 315:370–373, 2007.
7. C. P. Broedersz, M. Depken, N. Y. Yao, M. R. Pollak, D. A. Weitz, and F. C. MacKintosh. Cross-link governed dynamics of biopolymer networks. *Phys. Rev. Lett.*, 105:238101, 2010.
8. M. Fortin and D. Esselaoui. A finite-element procedure for viscoelastic flows. *Int. J. Numer. Meth. Fluids*, 7(10):1035–1052, 1987.
9. J. Étienne, E. J. Hinch, and J. Li. A Lagrangian–Eulerian approach for the numerical simulation of free-surface flow of a viscoelastic material. *J. Non-Newtonian Fluid Mech.*, 136:157–166, 2006.
10. D. Ambrosi, A. Duperray, V. Peschetola, and C. Verdier. Traction patterns of tumor cells. *J. Math. Biol.*, 58:163–181, 2009.
11. D. Mitrossilis, J. Fouchard, A. Guiroy, N. Desprat, N. Rodriguez, B. Fabry, and A. Asnacios. Single-cell response to stiffness exhibits muscle-like behavior. *Proc. Natl. Acad. Sci. USA*, 106:18243–18248, 2009.
12. D. Mitrossilis, J. Fouchard, D. Pereira, F. Postic, A. Richert, M. Saint-Jean, and A. Asnacios. Real-time single cell response to stiffness. *Proc. Natl. Acad. Sci. USA*, 107:16518–16523, 2010.
13. O. M. Rossier, N. Gauthier, N. Biais, W. Vonnegut, M.-Antoine Fardin, P. Avigan, E. R Heller, A. Mathur, S. Ghassemi, M. S Koeckert, J. C Hone, and M. P. Sheetz. Force generated by actomyosin contraction builds bridges between adhesive contacts. *EMBO J.*, 29:1033–1044, 2010.